

Recent Applications of (e, 2e) Techniques*

M. J. Brunger

Physics Department, Flinders University of South Australia,
GPO Box 2100, Adelaide, SA 5001, Australia.

Abstract

The flexibility of the (e, 2e) technique in obtaining information on both structure and collision dynamics is demonstrated. An example of the structure information that can be obtained is illustrated by electron momentum spectroscopy studies on krypton, while the role of post-collision effects and correlations is explored by measurements in the autoionising region of helium.

1. Introduction

The (e, 2e) process, in which the momenta of the incident electron and two emitted electrons in an ionising collision are completely determined, is capable of revealing a rich variety of information. Depending on the kinematics employed, it is possible to investigate in detail either the dynamics of the ionising collision or to use the reaction to elucidate the structure of the target and the ion. When used for structure determination, high energies and high momentum transfers are normally employed to ensure the ‘clean’ knockout of a target electron. This form of (e, 2e) spectroscopy, where the kinematics are symmetric, is commonly referred to as electron momentum spectroscopy (EMS) and has been reviewed extensively by McCarthy and Weigold (1988, 1991) and more recently by Brion (1993) and Coplan *et al.* (1994).

For most ionising collisions, however, the kinematics is asymmetric, the two outgoing electrons having very different energies and the momentum transfer to the target is usually small. Such asymmetric collisions have generally been studied using simple targets such as hydrogen (Weigold *et al.* 1979) or helium (Ehrhardt *et al.* 1972; Avaldi *et al.* 1987; Hawley-Jones *et al.* 1992; Lubell 1994) whose structure is known or assumed to be known in order to test our understanding of the ionisation mechanism. As the momentum transfer approaches zero, the (e, 2e) reaction simulates photo-ionisation, and this kinematic region has been used to obtain useful information on partial oscillator strengths (e.g. Hamnett *et al.* 1976).

The (e, 2e) reaction has also been used to investigate final state correlation effects between the continuum electrons. This has mainly focussed on post collision

* Refereed paper based on a contribution to the Advanced Workshop on Atomic and Molecular Physics, held at the Australian National University, Canberra, in February 1995.

interaction effects (PCI) in the ionisation of inner shells resulting in the emission of Auger electrons, particularly the ionisation of the 2p shell of argon (Sewell and Crowe 1982, 1984; Sandner and Völkel 1984; Stefani *et al.* 1986; Lohmann 1991; Lohmann *et al.* 1992; Waterhouse *et al.* 1993; Bell *et al.* 1993; Kuchiev and Sheinerman 1994). The reaction has also been used to study the correlations between resonance and direct ionisation amplitudes in the autoionising region of helium e.g. Weigold *et al.* (1975*b*), Pochat *et al.* (1982), Kuchiev and Sheinerman (1989, 1994), Lower and Weigold (1990), McDonald and Crowe (1992, 1993), McCarthy and Shang (1993), Kheifets (1993), and Samardzic *et al.* (1994, 1995).

In this communication I discuss briefly a few (e,2e) studies recently carried out at the Flinders University of South Australia. These include the first high accuracy EMS study of the satellite structure of the krypton valence shell at 1000 eV and the measurement of correlation effects in the autoionising region of helium.

2. Theory

The (e,2e) reaction can be written

$$e_0 + A \rightarrow A_f^+ + e_S + e_e, \quad (1)$$

where the subscripts 0, S and e denote the incident, scattered and ejected electrons respectively. Although the two emitted electrons are indistinguishable, it is often convenient to call the 'fast' outgoing electron the scattered one and the other the ejected one. Conservation of energy and momentum requires

$$\epsilon_f = E_0 - E_S - E_e, \quad (2)$$

$$\mathbf{k}_0 = \mathbf{k}_S + \mathbf{k}_e - \mathbf{q}, \quad (3)$$

where ϵ_f , the separation (or binding) energy of the electron, is equal to the energy difference between the initial target state A and the final state $|f\rangle$ of the ion. The recoil momentum of the ion is denoted by $-\mathbf{q}$ and in the plane wave impulse approximation (PWIA), $-\mathbf{q}$ is simply the momentum of the struck (bound) electron (\mathbf{p}). The ion recoil energy has been neglected. The momentum transfer to the target is given by

$$\mathbf{K} = \mathbf{k}_0 - \mathbf{k}_S. \quad (4)$$

In noncoplanar and coplanar symmetric (e,2e) experiments K is maximised by choosing $k_e = k_S$ and $\theta_e = \theta_S$, where θ_e and θ_S are the ejected and scattered electron scattering angles.

For the EMS experiments I describe in Section 4, the PWIA is generally used to analyse the measured cross sections. In this approximation, and within the Born–Oppenheimer approximation, the (e,2e) differential cross section σ for randomly oriented molecules is given by

$$\sigma = M \int dv \int d\Omega | \langle e^{i\mathbf{p}\cdot\mathbf{r}} \Psi_f^{N-1} | \Psi_i^N \rangle |^2, \quad (5)$$

where M is a kinematical factor which is essentially constant in the present experimental arrangement, Ψ_f^{N-1} and Ψ_i^N are the many body wavefunctions for the final ($(N-1)$ electron) ion and initial (N electron) neutral states, $\int d\Omega$ denotes an integral over all angles (spherical averaging) due to the averaging over all initial rotational states and $\int dv$ an integral over the initial vibrational states, which is usually well approximated by evaluating wavefunctions at the equilibrium geometry of the molecule. The momentum space ion-molecule overlap, $\langle e^{i\mathbf{p}\cdot\mathbf{r}}\Psi_f^{N-1} | \Psi_i^N \rangle$, can be evaluated directly but often the target Hartree-Fock approximation (THFA) is made in which Ψ_i is replaced by the Hartree-Fock ground state Φ_i . Under the THFA and the equilibrium geometry approximation equation (5) reduces (McCarthy and Weigold 1991) to

$$\sigma = MS_j^{(f)} \int d\Omega_f |\phi_j(\mathbf{p})|^2, \quad (6)$$

where $\phi_j(\mathbf{p})$ is the momentum space wavefunction for the Hartree-Fock orbital j from which the electron was ionised. It is thus transparent from equation (6) why the EMS technique has the capability for wavefunction mapping. The spectroscopic factor $S_j^{(f)}$ is the probability of finding the one-hole configuration j in the expansion of the final ion state, and satisfies the sum rule

$$\sum_f S_j^{(f)} = 1. \quad (7)$$

In Section 5 we describe the results of some of our experiments that investigate autoionisation phenomena in He. In this discussion we compare the derived experimental quantities f , a and b with those correspondingly calculated by Kheifets (1993). It is thus appropriate that we now provide a brief description of this calculation.

The triple differential cross section near an isolated autoionisation resonance in the (e, 2e) energy spectrum of ejected electrons can be parametrised by the formula (Shore 1967)

$$\frac{d^5\sigma}{d\Omega_e d\Omega_S dE_e} = f_r + \sum_{\mu} \frac{a_{\mu}\epsilon_{\mu} + b_{\mu}}{1 + \epsilon_{\mu}^2}, \quad (8)$$

where f_r is the non-resonant part of the triple differential cross section

$$\epsilon_{\mu} = 2(E_e - \bar{E}_{\mu})/\Gamma_{\mu} \quad (9)$$

and where \bar{E}_{μ} and E_e are respectively the energies of the r th autoionising resonance and the energy of the ejected electron, with total angular momentum and spin quantum numbers denoted by $\mu = (r; L, M, S)$. The energy full width at half maximum of the resonance is given by Γ_{μ} . Here \bar{E}_{μ} and Γ_{μ} are dictated by the configuration interaction of the discrete doubly excited states and are well known (see Table 1) for the states studied (van den Brink *et al.* 1989), while a_{μ} and b_{μ} are the momentum-dependent Shore parameters. These parameters have the units of a cross section and are assumed to be constant in the energy region

of the resonance: a_μ characterises the asymmetry of the resonance profile and is composed of an interference term between the direct and resonant ionisation amplitude: b_μ also contains an interference term and an additional term which yields the resonant cross section in the absence of any direct ionisation cross section (Lower and Weigold 1990).

Table 1. Energies (eV) and natural widths (eV) of the four autoionising states considered in the present work, as well as their corresponding ejected electron energies

The numbers in parentheses for the energies and widths are their one standard deviation uncertainties

State	\bar{E}_μ	Γ_μ	E_e
$(2s^2)^1S$	57.83(0.04)	0.138(0.015)	33.24
$(2s2p)^3P$	58.31(0.02)	0.008	33.72
$(2p^2)^1D$	59.91(0.02)	0.072(0.018)	35.32
$(2s2p)^1P$	60.145	0.038(0.002)	35.555

Following Kheifets (1993) we write f_r in terms of the singlet ($S' = 0$) and triplet ($S' = 1$) ionisation amplitudes,

$$f_r = N \sum_{S'} (2S' + 1) |T_{S'}(\mathbf{k}_0, \mathbf{k}_e, \mathbf{k}_S)|^2, \quad (10)$$

where the coefficient N depends on the normalisation and kinematics of the process under consideration, and S' is the total spin of the two outgoing electrons. The parameters a and b in equation (8) can be presented in the form similar to those of Tweed and Langlois (1986),

$$N^{-1}a = 2\text{Re}[T_{S'}^* t_\mu (q - i)], \quad (11)$$

$$N^{-1}b = 2\text{Im}[T_{S'}^* t_\mu (q - i)] + |t_\mu (q - i)|^2,$$

with the coefficient N of equation (10). Here the resonant amplitude t_μ is the ionisation amplitude to the open channel in which the resonance occurs. The Fano profile index q entering equation (11) is given by

$$q = \left(\frac{1}{2} \pi \Gamma_\mu \right)^{-\frac{1}{2}} \frac{\tau_\mu}{t_\mu}, \quad (12)$$

where τ_μ is the resonance excitation amplitude. Note that in the Kheifets (1993) calculation the non-resonant ionisation and resonance excitation amplitudes were calculated in the distorted wave Born approximation (DWBA) scheme.

In order to include the long-range Coloumb interaction in the final state the amplitude $T_{S'}$ is multiplied by the Gamow factor,

$$C(\eta)e^{i\delta_0} = \frac{2\pi\eta}{e^{2\pi\eta} - 1} e^{i \arg \Gamma(1-i\eta)}, \quad (13)$$

where $\eta = |\mathbf{k}_e - \mathbf{k}_S|^{-1}$ is the inverse relative momentum of the two outgoing electrons.

The parameters a and b contain the complex amplitudes $T_{S'}$, t_μ and τ_μ and depend not only on their absolute values but also on their relative phases. Consequently it makes them extremely sensitive both to the dynamics of the reaction and the structure of the atomic target being ionised. Thus the measurement of these parameters offers a rigorous test to the theory of atomic ionisation by electron impact.

3. Experimental Details

The electron-coincidence spectrometer and the techniques used in the present EMS investigation of the satellite structure of krypton have been described in some detail previously by McCarthy and Weigold (1991), and so in the interests of brevity we do not go into detail here. The only major recent change to the non-coplanar symmetric coincidence spectrometer has been the inclusion of a differentially pumped collision chamber. The high purity krypton is admitted into the target chamber through a capillary tube, the leak rate being controlled by a variable leak valve. The collision region is surrounded by a chamber pumped by a $700 \ell s^{-1}$ diffusion pump. Apertures and slits are cut in the collision chamber for the incident beam and ejected electrons. The differentially pumped collision region makes it possible to increase the target gas density by a factor of two while keeping the background pressure in the spectrometer below 10^{-5} Torr. This allowed us to operate the electron beam at a lower current (typically $40 \mu A$) resulting in a better energy resolution. The energy resolution of the present measurements is 1.25 eV (FWHM), and the angular resolution is 1.2° (FWHM). Operating conditions were chosen so that the incident energy $E_0 = 1000$ eV + separation energy, the ejected electrons had energies E_S and E_e in the range 500 ± 7 eV and made angles of $\theta_S = \theta_e = 45^\circ$ with respect to the incident electron beam direction. The out-of-plane azimuthal angle ϕ was chosen to be either $\phi = 0^\circ$ or $\phi = 8^\circ$ in order to vary the recoil momentum as

$$p = [(2p_S \cos \theta - p_0)^2 + 4p_S^2 \sin^2 \theta \sin^2 \phi/2]^{\frac{1}{2}}. \quad (14)$$

Separation energy spectra were taken at each of the two out-of-plane azimuthal angles over the range $\epsilon_f = 9\text{--}42$ eV using the binning mode (McCarthy and Weigold 1988).

For the autoionisation studies in helium the apparatus and multiparameter coincidence techniques used were described in detail previously by Lower and Weigold (1989, 1990) and so, as above, only a brief description is now presented. The (e, 2e) coincidence spectrometer consists of two hemispherical analysers which determine the energy of the scattered and ejected electrons. Each is fitted with a decelerating and focussing lens system and employs a position sensitive detector to enable simultaneous measurement over a broad range of electron energies. Furthermore, each hemispherical analyser had fringe-field correcting rings inserted between the inner and outer hemispheres and a narrow exit slit between the analyser exit plane and channel plate detector, to ensure we closely mimicked an ideal field case. These precautions minimised ($< 1\%$) the degree of non-linearity in the energy dispersion of the hemispherical analysers so that no corrections to the energy scale were required (Lower and Weigold 1990).

The analysers are each mounted on an independently rotatable turntable, concentric with the axis of the gas beam and their angular positions can be adjusted through computer controlled stepping motors. The target beam effuses through a 15 mm long molybdenum tube of internal diameter 0.7 mm, before proceeding through a collimating aperture. Positioned behind the interaction region is the electron gun. The present gun has aperture-type lens elements and was designed on the basis of the model calculations of Harting and Read (1976). Significantly, it produced an intense (typically $I_{\text{cup}} \sim 14 \mu\text{A}$) well collimated electron beam of well defined energy and momentum. This beam was monitored and focussed into a small Faraday cup. The intersection between the electron and helium beams defined the interaction region. The apparatus was configured for coplanar geometry, meaning the incident electron beam and the scattered and ejected electrons all share a common plane. In this configuration the two outgoing electrons leave the collision centre at angles θ_S and θ_e with respect to the incident beam direction. The angle $\phi = \phi_e - \phi_S$ is restricted to a value of π (binary collision region), corresponding to the condition where both analysers are positioned on opposite sides of the incident beam. In the present work the energy of the incident beam was either 94.6 eV, 96.6 eV or 99.6 eV. One analyser measured 'ejected' electrons over a range of energies between 32 and 37 eV, a region encompassing the $(2s^2)^1S$, $(2s2p)^3P$, $(2p^2)^1D$ and $(2s2p)^1P$ resonant states. 'Scattered' electrons were collected in the second analyser over a complementary 5 eV range, the position of which was determined by energy conservation. In the present series of work the scattered electron analyser was fixed at either $\theta_S = 30^\circ$ or 20° , respectively, whilst the coincidence ejected electron spectra were measured over the range -25° to -135° of ejection angles θ_e . Each measurement involved repeated scans through the angular range of the ejected electron analyser, to average over beam and target density fluctuations and long term instrumental drifts. The integrated count rate from the fixed scattered electron analyser was used as a preset to determine the dwell-time of each angular position.

The coincidence circuitry and its optimisation are discussed thoroughly by Lower and Weigold (1989) to which the reader is referred for more detail.

4. Satellite Structure of the Krypton Valence Shell by EMS

In recent times the study of correlation satellites in ionisation spectra of rare gas atoms has been the subject of renewed interest (Krause *et al.* 1992). There are at least three reasons for this:

- (1) The advancement of theoretical and computational methods is now giving reliable results for pole strengths for the most prominent low-energy satellites (Amusia and Kheifets 1991; Fronzoni *et al.* 1992).
- (2) The experimental development of atomic and molecular physics at an increasing number of synchrotron radiation centres makes feasible photoionisation studies of gases at low pressures with synchrotron radiation of variable photon energy (Svensson *et al.* 1988).
- (3) The measured spectroscopic factors of satellites in EMS valence electron spectra are independent of the incident energy and the target electron momentum, but differ from the corresponding photoelectron spectroscopy (PES) values, which are energy dependent even at high momentum (McCarthy and Weigold 1991).

Whereas there have been a large number of EMS and PES measurements and theoretical calculations for the valence electronic structure of neon, argon and xenon (see, for example, Samardzic *et al.* 1993; McCarthy *et al.* 1989; Braidwood *et al.* 1993; Brunger *et al.* 1994 and references therein), the same cannot be said for krypton. The earliest EMS studies for evidence of correlation effects in the separation energy spectra of krypton were made by Weigold *et al.* (1975a) and Fuss *et al.* (1981). Both these studies suffered from the limited statistical accuracy inherent with single channel coincidence measurements and from energy resolution $\Delta E_{\text{coin}} \geq 2$ eV, which effectively 'smeared out' the 4s valence satellite structure. Leung and Brion (1983) also independently measured, in an EMS experiment, the 4p and 4s satellite structure of krypton, but again this was a single channel measurement so that the statistical quality of their data was only fair. We note, however, that they improved the energy resolution of their work so that $\Delta E_{\text{coin}} = 1.6$ eV which, whilst being clearly superior to Fuss *et al.* (1981), was, in the context of resolving the 4s satellite structure, of only marginal quality. Indeed Leung and Brion (1983) specifically called for a further measurement of the krypton inner valence shell, with better energy resolution and improved statistics, to better define the 4s satellite structures. The results of just such a study, which have been made possible by employing multiparameter techniques, are reported here. PES investigations have also found significant satellite structure for the krypton valence shell. In this regard we note the early study of Spears *et al.* (1974) and the more recent, extensive, investigations of Svensson *et al.* (1988) and Krause *et al.* (1992). From a theoretical perspective Dyall and Larkins (1982*a, b*) have applied their frozen-core CI model to calculate the satellite spectra of krypton (amongst others) up to separation energies of 43 eV. More exact calculations for the 4p and 4s satellite states have been provided by Fronzoni *et al.* (1992) and Brosolo *et al.* (1992) who employed a two hole-one particle (2h-1p) CI calculation scheme.

The binding energy spectrum of krypton in the region ~ 9 –42 eV is shown in Fig. 1 for a total energy of 1000 eV and with the out-of-plane azimuthal angles $\phi = 0^\circ$ and $\phi = 8^\circ$. Also shown is the summed spectrum for $\phi = 0^\circ + 8^\circ$. At $\phi = 0^\circ$ the momentum p ranges from 0.159 a.u. at the binding energy of the first peak ($\epsilon_f = 14.11$ eV) to 0.184 a.u. for $\epsilon = 40.47$ eV. At 8° the corresponding momenta are 0.615 and 0.623 a.u. respectively. Note that the first peak in Fig. 1 is actually a convolution of the $J = \frac{3}{2}$ and $J = \frac{1}{2}$ components of the 4p line. However, as these spin-orbit split states are only separated by 0.67 eV, the coincident energy resolution of the present experiment did not allow the two components to be resolved. The spectra in Fig. 1 show satellites not previously observed in EMS, although all of them have been reported in the extensive PES studies of Svensson *et al.* (1988) and Krause *et al.* (1992).

Considering Fig. 1 in more detail than at $\phi = 0^\circ$, i.e. at low momenta, the 4p ground-state cross section is some 48% of that for the main $4s^{-1}$ transition ($4s^1 4p^6$) at 27.52 eV, whereas at $\phi = 8^\circ$ its cross section is $2\frac{1}{2}$ times that of the 27.52 eV transition. Thus any reasonable 2P satellite intensity in the range 9–42 eV should be noticeable in Fig. 1 by peaks which are somewhat stronger at $\phi = 8^\circ$ than at $\phi = 0^\circ$. To aid in this comparison the relative intensities of the peaks in Fig. 1, as well as their separation energies, are given in Table 2. Note that the intensities in this table are relative to the $\phi = 0^\circ$ ($4s^1 4p^6$) $4s^{-1}$

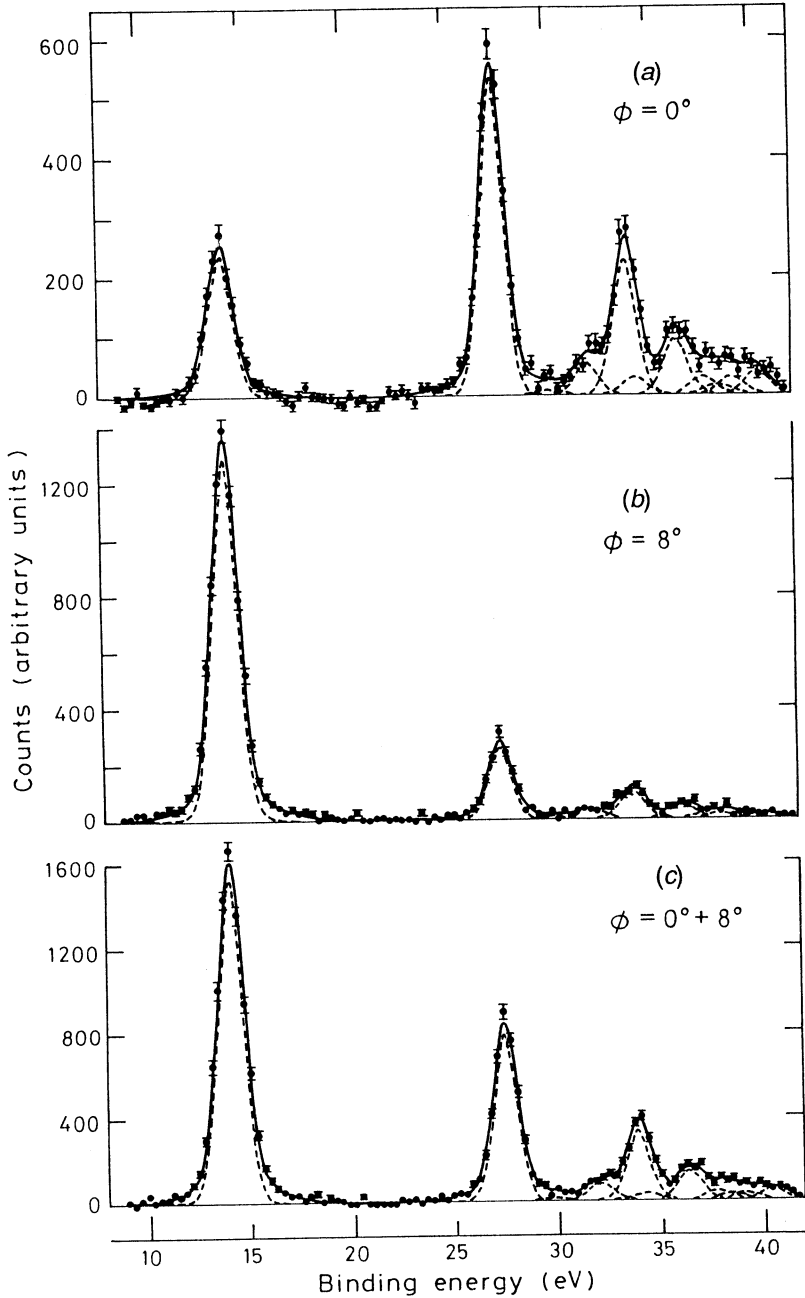


Fig. 1. The 1000 eV non-coplanar symmetric EMS separation energy spectra for krypton at (a) $\phi = 0^\circ$, (b) $\phi = 8^\circ$ and (c) $\phi = 0^\circ + 8^\circ$. The curves show the fitted spectra using the known resolution function.

transition at 27.52 eV which is arbitrarily set to 100. It is apparent that, aside from the main $(4s^2 4p^5)4p^{-1}$ line at $\epsilon_f = 14.11$ eV, the only other candidate for membership of the 2P manifold is peak 3 at $\epsilon_f = 30.25$ eV. On the other hand, satellites belonging to the 2S manifold should have a much larger cross section

at $\phi = 0^\circ$ compared to that at $\phi = 8^\circ$. Peak 2 and peaks 4–11 of Fig. 1 clearly correspond to this behaviour. Note that the intensities from the high energy PES results of Svensson *et al.* (1988) and the low energy data of Krause *et al.* (1992) are not included in Table 2. This is due to the fact that there are obviously big differences in the satellite intensities between these PES data, thus making them somewhat difficult to interpret.

Table 2. Peak energies and relative intensities of the 1000 eV spectra shown in Fig. 1

The intensities are relative to a value of 100 for the $\epsilon_f = 27.52$ eV transition at $\phi = 0^\circ$

Peak	ϵ_f (eV)	$\phi = 0^\circ$	$\phi = 8^\circ$
1	14.11	48.13	254.10
2	27.52	100.00	49.05
3	30.25	1.15	1.37
4	32.09	10.36	5.61
5	33.98	41.70	18.97
6	34.47	6.15	0.53
7	36.47	18.08	9.05
8	37.81	6.22	2.69
9	38.57	3.18	2.11
10	39.21	5.99	2.11
11	40.47	7.89	2.97

In attempting to assign configurations for the transitions 1–11 of Fig. 1 and Table 2, we made use of the calculations of Dyllal and Larkins (1982*a, b*) and Fronzoni *et al.* (1992), as well as the PES results of Svensson *et al.* (1988) and Krause *et al.* (1992). A summary of our classifications for the final-state configurations of the 2S and 2P manifolds of Kr that we observed, and the spectroscopic factors derived from the present EMS spectra, are given in Table 3. Also shown in this table are the PES results of Svensson *et al.* (1988) and Krause *et al.* (1992), the previous EMS result of Fuss *et al.* (1981), and the calculated results of Dyllal and Larkins (1982*a, b*) and Fronzoni *et al.* (1992) and Brosolo *et al.* (1992). Note, as Amusia and Kheifets (1991) found that the PES cross section was not proportional to the ‘true’ spectroscopic factor we would, *a priori*, not expect to find a significant correspondence between the EMS (see equation 6) and PES results for $S_j^{(f)}$.

The first peak in Fig. 1 at $\epsilon_f = 14.11$ eV is, as discussed earlier, a convolution of the $J = \frac{3}{2}$ and $J = \frac{1}{2}$ $4p^{-1}$ lines with configuration $4s^24p^5 \ ^2P$. The present EMS separation energy is in good accord with the PES value of Svensson *et al.*, although we observe that the calculation of Fronzoni *et al.* underestimates its correct value. In terms of the spectroscopic factors for this pole we see in Table 3 that there is quite good agreement between the present result and the PES result of Svensson *et al.* the previous EMS result of Fuss *et al.* (1981) and the calculation of Dyllal and Larkins (1982*a, b*). Note that the present values of $S_j^{(f)}$ at $\phi = 0^\circ$ and 8° are consistent with one another (a trend found for all states 1–11) showing the EMS spectroscopic factors are independent of momentum. The second peak in Fig. 1 is clearly due to the main $4s^{-1}$ line with dominant configuration $4s^14p^6 \ ^2S$. Both the PES studies and the present EMS

determination of $\epsilon_f = 27.52$ eV for this pole are in good accord. This is not the case, however, for the spectroscopic factors where the PES result of Svensson *et al.* and the calculation of Dyllal and Larkins clearly overestimate its strength (see Table 3). On the other hand the 2h-1p calculation of Fronzoni *et al.* is in much better accord with the present determination of $S_j^{(f)}$ for this pole, whilst the earlier EMS result is in reasonable agreement, albeit somewhat smaller, with the present result. Peak 3 at $\epsilon_f = 30.25$ eV is a very weak satellite which, on the basis of our result in Table 2, appears non 's-like' in symmetry. Both Svensson *et al.* and Krause *et al.* observed a line at this separation energy which they classified as having the configuration $4s^24p^4(^3P) 4d\ ^2P$. The current EMS result is certainly consistent with that interpretation and we believe that this is the first time a satellite of 2P symmetry, other than the main 2P line, has been observed in an EMS experiment. The pole at $\epsilon_f = 32.09$ eV is 's-like' in symmetry and we have assigned it to be the lowest order member ($n = 5$) of the Rydberg series of final ion states with configurations $4s^24p^4(^1S) (5, 6, \dots)s\ ^2S$. This assignment is consistent with those of the PES measurements of Svensson *et al.* and Krause *et al.* The present spectroscopic factor for this pole is in good accord with the earlier EMS determination of Fuss *et al.*, but is somewhat stronger than that measured by Svensson *et al.* and calculated by Fronzoni *et al.* and Dyllal and Larkins.

A very strong satellite (peak 5) is also observed in the separation energy spectrum at $\epsilon_f = 33.98$ eV. This peak possesses s-like symmetry and, again consistent with the PES classification, we assign it to be the lowest order member ($n = 4$) of the Rydberg series of final ion states with configuration $4s^24p^4(^1D) (4, 5, 6, 7, \dots)d\ ^2S$. Agreement, in terms of the position of the satellite in the separation energy spectrum, between PES and the current EMS measurement is good. Similarly, the present EMS value for the spectroscopic factor is in good agreement with the earlier work of Fuss *et al.* and with the 2h-1p result of Fronzoni *et al.* The PES determination and the calculation of Dyllal and Larkins were found to somewhat underestimate the strength of this pole. At $\epsilon_f = 34.47$ eV we find a state (peak 6) of s-like symmetry which we have classified, in good agreement with that of Krause *et al.* (1992), as being the $n = 6$ member of the series $4s^24p^4(^1S) ns\ ^2S$. On the other hand this classification is at odds with that originally proposed by Svensson *et al.* who mistakenly assigned this satellite with the configuration $4s^24p^4(^3P) 6p\ ^2P$. It is possible that there could be some 'p-like' intensity at this value of separation energy, but such a p-component is obviously very small and consequently obscured by the s-contribution. Peaks 7-11 of Fig. 1 are the $n = 5, 6, 7, 8$ and ≥ 9 poles of the Rydberg series $4s^24p^4(^1D) nd\ ^2S$. This classification scheme is again consistent with the PES results. Furthermore, for these satellites we highlight the fairly good level of agreement between the present EMS result and the calculations of Fronzoni *et al.* (1992), Dyllal and Larkins (1982a, b) and the PES measurement of Svensson *et al.* (1988) in most cases.

Finally we note that it is apparent from Table 3 that there are quite a few satellites observed in the PES spectra that are not identified in the current EMS measurements. These satellites are of 2P and 2D manifold symmetry and are very weak in intensity (see Svensson *et al.* 1988). Consequently they are dominated, in the EMS experiment, by the 2S satellites in their vicinity and thus are not seen.

Table 3. Spectroscopic factors and final-state configurations for the 4p and 4s manifolds of krypton as determined from the relative (e, 2e) differential cross sections at 1000 eV for $\phi = 0^\circ$ and $\phi = 8^\circ$

The one standard deviation error in the last significant figure is given in parentheses

Line	Binding energy (eV)		$\Gamma(\text{FWHM})^{(a)}$	Assignment ^(a,b)	(a)	(c)	(d)	$S_i^{(f)}$	
	(b)	(c)						Present EMS	$\phi = 0^\circ$
4p _{3/2}	14.00	12.50	0.49	4s ² 4p ⁵ 2P	0.964	0.910	~1	0.978	0.977(20) 0.990(10)
4p _{1/2}	14.67	—	0.49	—	—	—	—	—	—
27.52	27.51	24.96	0.49	4s ¹ 4p ⁶ 2S	0.658	0.564	0.46(2)	0.69	0.501(10) 0.527(20)
29.83	29.83	—	—	(¹ D)5s 2D	—	—	—	—	—
30.25	30.28	30.25	0.49	4s ² 4p ⁴ (³ P)4d 2P	—	—	—	—	0.023(15) 0.010(10)
30.69	30.69	—	—	(³ P)4d 2D _{3/2}	—	—	—	—	—
30.98	30.98	—	—	(³ P)4d 2D _{5/2}	—	—	—	—	—
31.25	31.29	—	0.58	4s ² 4p ⁴ (³ P)5p 2P	0.011	0.006	—	0.002	—
31.65	31.65	29.46	—	(³ P)5p 2S	—	—	—	—	—
32.09	32.06	30.18	0.55	4s ² 4p ⁴ (¹ S)5s 2S	0.015	0.027	0.07(2)	0.024	0.052(5) 0.060(10)
32.75	32.61	30.98	0.55	4s ² 4p ⁴ (¹ D)5p 2P _{3/2,1/2}	0.024	0.058	—	0.011	—
32.88	32.88	—	—	—	—	—	—	—	—
33.98	33.96	32.54	0.55	4s ² 4p ⁴ (¹ D)4d 2S	0.157	0.196	0.20(2)	0.141	0.209(7) 0.204(9)
34.14	34.14	—	—	(³ P)6s 2P	—	—	—	—	—
34.38	34.38	34.47	—	(¹ S)6s 2S	—	—	—	0.013	0.030(10) 0.010(20)
34.47	34.47	32.92	0.5	4s ² 4p ⁴ (³ P)6p 2P	0.006	0.015	—	0.002	—
34.74	34.74	—	—	?	—	—	—	—	—
34.9	34.89	32.75	0.55	4s ² 4p ⁴ (¹ S)5p 2P _{1/2,3/2}	0.006	0.001	—	0.003	—
34.93	34.93	—	—	?	—	—	—	—	—
35.14	35.14	—	—	?	—	—	—	—	—
35.85	35.85	—	—	(¹ D)5d 2D _{3/2}	—	—	—	—	—
36.12	36.12	—	—	(¹ D)5d 2P _{1/2}	—	—	—	—	—
36.47	36.47	34.79	0.55	4s ² 4p ⁴ (¹ D)5d ² S+(¹ D)6p	2P	0.070	0.084	0.089	0.090(6) 0.097(8)
36.70	36.70	34.49	—	?	—	—	—	—	—
37.65	37.65	—	—	?	—	—	—	—	—
37.81	37.82	36.09	0.55	4s ² 4p ⁴ (¹ D)6d	2S	0.033	0.046	0.036	0.031(4) 0.029(7)
38.57	38.58	36.76	0.60	4s ² 4p ⁴ (¹ D)7d	2S	0.020	0.019	—	0.016(4) 0.022(6)
39.21	39.04	37.26	~1	4s ² 4p ⁴ (¹ D)8d	2S	—	0.005	—	0.030(5) 0.022(7)
39.77	39.33	38.18	~1	4s ² 4p ⁴ (¹ D)nd, n ≥ 9	2S	0.011	0.014	—	0.039(3) 0.032(5)
39.53	39.53	40.47	—	—	—	—	—	—	—

(a) Svensson *et al.* (1988) ($h\nu = 1487$ eV). (b) Krause *et al.* (1992) ($h\nu = 68.5$ eV). (c) Fronzoni *et al.* (1992) (2h-1p CI calculation) and Brosolo *et al.* (1992) (2h-1p CI calculation). (d) Fuss *et al.* (1981), experiment. (e) Dyllal and Larkins (1982a, b).

5. (e, 2e) Coincidence Measurements in the Autoionising Region of Helium

The autoionisation of atoms by electron impact involves in general the interference between the direct and resonance ionisation amplitudes. This interference depends on the momenta of the scattered and ejected electrons and on the momentum transfer. Therefore (e, 2e) cross section measurements in the autoionising region can provide very sensitive information on details of the excitation process of the resonance as well as on the interference of the resonance process with direct ionisation.

Fig. 2 provides some examples of the observed coincidence ejected electron spectra (Samardzic *et al.* 1995). We see a series of resonance profiles superimposed upon a background of direct ionisation events. Each individual resonance is fitted, in a least-squares fit analysis, with the profile $a\epsilon + b/1 + \epsilon^2$ (see equations 8 and 9), convolved with the instrumental response, whilst the direct ionisation cross section f is represented by a linear function in the fit. The final fitted function is denoted by the solid curve in each diagram. Both of the spectra were obtained in the binary region with the only difference being 15° in the ejected electron angle. This is a clear demonstration of how sensitive the cross sections are to the ejected electron momentum.

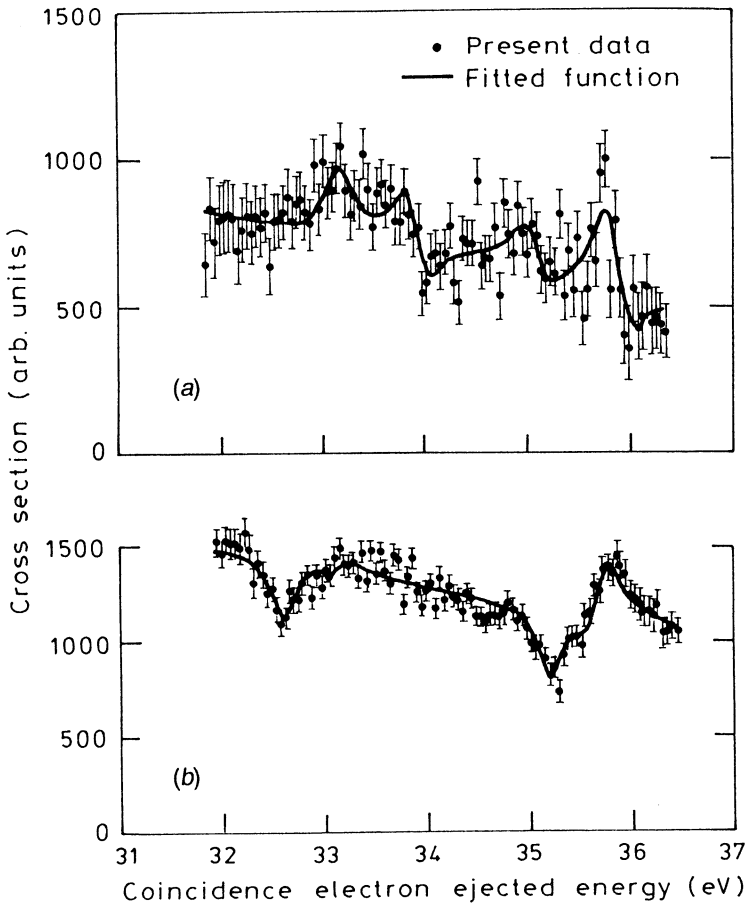


Fig. 2. Coincidence ejected electron spectra for $\text{He}(e, 2e)\text{He}^+$ $E_0 = 94.6$ eV, $E_S = 35$ eV, $E_e = 35$ eV and $\theta_S = 30^\circ$ for the ejected electron angles (a) $\theta_e = -25^\circ$ and (b) $\theta_e = -40^\circ$.

Values for a_r , b_r and f_r deduced from the fitting of the individual coincidence ejected electron spectra for the $(2s^2)^1S$, $(2s2p)^1P$ and $(2p^2)^1D$ resonances, in general, show quite rapid variations as a function of θ_e . Fig. 3 shows the results of the angular dependence in a_r , b_r and f_r for the 1D state at $E_0 = 94.6$ eV with $E_S = 35$ eV, $E_e = 35$ eV and $\theta_S = 30^\circ$. Note that the present measurements do not determine cross sections on an absolute scale (although relative normalisations between states and angles are maintained) and hence the experimental and theoretical results required normalisation before comparison with each other. In this case we have normalised the data so that $f_{1S}(\theta_e = -40^\circ) = 1$. Also shown in Fig. 3 is the energy shift, $\Delta\epsilon$, due to post-collision-interaction (PCI) effects,

$$\Delta\epsilon_\mu = \bar{E}_\mu(e, 2e) - \bar{E}_\mu^{\text{true}}, \quad (15)$$

which we also report as a function of θ_e . It is clear from equation (15) that $\Delta\epsilon_\mu$ can be either positive or negative depending on whether the position of the resonance in the (e, 2e) spectra appears at a higher or lower value of energy with respect to the corresponding resonance energy in the double differential cross section spectra. The phenomenon of PCI arises due to the Coulomb interaction between a number of charged particles in the collision systems final state, with the Coulomb interaction being thought of as 'post-collisional' in the sense that the reaction occurs in two stages via an intermediate resonance. An excellent review of PCI can be found in Kuchiev and Sheinerman (1989) and in their more recent paper (Kuchiev and Sheinerman 1994) and so we do not go into detail here, except to note that PCI can affect the experimental coincident ejected electron spectra by one or both of:

- (1) a positive or negative shift ($\Delta\epsilon$) in the apparent position of the resonance energy;
- (2) a broadening of the apparent full width at half maximum Γ of the resonance.

In Fig. 3 the results of the calculation based on the DWBA + exchange model of Kheifets (1993), as discussed earlier in Section 2 of this paper, are also plotted. The level of agreement between theory and experiment for the a_r and b_r parameters of the 1D resonance is seen to be quite good over the measured angular range, in terms of both the shape and magnitude of the parameters. Note that the a_r and b_r parameters show smooth oscillation between positive and negative values as the ejection angle varies. Positive values of b_r correspond to constructive interference between direct and resonant ionisation amplitudes, resulting in localised increases in the (e, 2e) cross section. Negative values of b_r are related to a decrease in the cross section due to the effect of destructive interference. For the f -parameter we also show the result of the DWBA + Gamow calculation and, whilst it is clear that this gives an arguably better description of the direct ionisation reaction mechanism than does the DWBA + exchange calculation, the DWBA + exchange result is still seen to be adequate. In the case of $\Delta\epsilon$ we see that the evidence for PCI effects is not definitive. At most angles, to within the experimental uncertainty in its determination, $\Delta\epsilon$ is very close to zero. This is not to say that PCI effects are absent in the excitation of the 1D state, they are clearly just quite small.

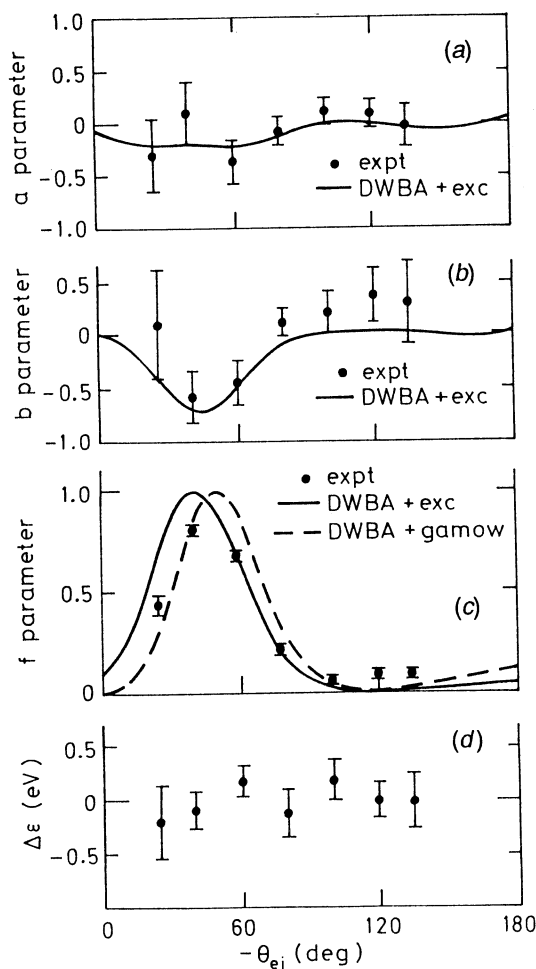


Fig. 3. Angular dependence for (a) a_r , (b) b_r , (c) f_r and (d) $\Delta\epsilon$ as a function of ejected electron angle. Here $E_0 = 94.6$ eV, $E_S = 35$ eV, $E_e = 35$ eV and $\theta_S = 30^\circ$; 1D state.

Fig. 4 makes the same sort of comparison, again for the 1D resonance, as did Fig. 3 except that now the kinematical conditions are $E_0 = 99.6$ eV, $E_S = 40$ eV, $E_e = 35$ eV and $\theta_S = 20^\circ$ (Brunger *et al.* 1996). Similar comments to those above for the data of Fig. 3 are also applicable here. In this case we have shown these data to simply highlight the fact that the theory can provide an adequate description of the reaction mechanism over a range of kinematical conditions and not just for those pertaining to the data of Fig. 3.

Although we have only shown data for the 1D state, it is generally true that the results for all three resonances show strong interference effects, both constructive and destructive, between the direct and resonance amplitudes. The resonance parameters show even more rapid variation in magnitude as a function of the ejected electron angles than does the direct cross section. Note that whilst the peak structures in a_r and b_r are in some sense correlated with the direction of the

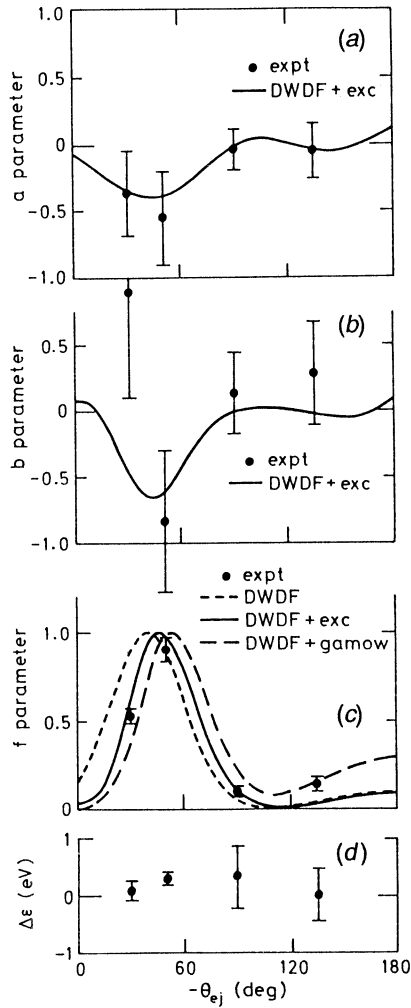


Fig. 4. Angular dependence for (a) a_r , (b) b_r , (c) f_r and (d) $\Delta\epsilon$ as a function of ejected electron angle. Here $E_0 = 99.6$ eV, $E_S = 40$ eV, $E_e = 35$ eV and $\theta_S = 20^\circ$; 1D state.

momentum transfer θ_K , as is that for the direct cross section f_r , the correlation is not simple. The calculation of Kheifets (1993) was found to be in fair agreement with experiment, in its predicted angular dependence for the parameters a_r , b_r and f_r , for the kinematical conditions of the present series of experiments.

6. Summary

The richness of information that can be obtained by the application of the (e, 2e) technique has been demonstrated by discussing a couple of different types

of experiments. One example involved the determination of structure information in a kinematic region where the (e,2e) collision process is well understood. The other involved the determination of subtle effects on the collision dynamics.

Acknowledgments

I wish to thank all the people involved in this work including Sean Braidwood, Anatoli Kheifets, Wolfgang von Niessen, Erich Weigold, Bo Shang, Anne-Marie Grisogono, Ian McCarthy, Jo Hurn and Olivia Samardzic. I also thank Karen Surfleed for continuing to type my appalling handwriting. I acknowledge the ARC for their financial support of some aspects of this work and also the organising committee of the Advanced Workshop on Atomic and Molecular Physics for their travel grant.

References

- Amusia, M. Ya., and Kheifets, A. (1991). *Aust. J. Phys.* **44**, 293.
- Avaldi, L., Camilloni, R., Fainelli, E., and Stefani, G. (1987). *J. Phys. B* **20**, 4163.
- Bell, S., Johnson, P., and Lohmann, B. (1993). Abstracts 18th Int. Conf. on the Physics of Electronic and Atomic Collisions, p. 213 (Aarhus University: Aarhus).
- Braidwood, S., Brunger, M. J., and Weigold E. (1993). *Phys. Rev. A* **47**, 2927.
- Brion, C. E. (1993). Proc. 18th Int. Conf. on the Physics of Electronic and Atomic Collisions, p. 350 (AIP Press: New York).
- Brosolo, M., Decleva, P., Fronzoni, G., and Lisini, A. (1992). *J. Mol. Struct. (Theochem.)* **26**, 233.
- Brunger, M. J., Braidwood, S. W., McCarthy, I. E., and Weigold, E. (1994). *J. Phys. B* **27**, L597.
- Brunger, M. J., Kheifets, A., Samardzic, O., Hurn, J., and Weigold, E. (1996). *J. Phys. B* **29**, in preparation.
- Coplan, M. A., Moore, J. H., and Doering, J. P. (1994). *Rev. Mod. Phys.* **66**, 985.
- Dyall, K. G., and Larkins, F. P. (1985a). *J. Phys. B* **15**, 203.
- Dyall, K. G., and Larkins, F. P. (1985b). *J. Phys. B* **15**, 219.
- Ehrhardt, H., Hesselbacher, K. H., Jung, K., Schultz, M., and Willmann, K. (1972). *J. Phys. B* **5**, 2107.
- Fronzoni, G., De Alti, G., Decleva, P., and Lisini, A. (1992). *J. Elect. Spectrosc. Relat. Phenom.* **58**, 375.
- Fuss, I., Glass, R., McCarthy, I. E., Minchinton, A., and Weigold E. (1981). *J. Phys. B* **14**, 3277.
- Hamnett, A., Stoll, W., Branton, G., Brion, C. E., and van der Wiel, M. J. (1976). *J. Phys. B* **9**, 945.
- Harting, E., and Read, F. H. (1976). 'Electrostatic Lenses' (Elsevier Scientific: Amsterdam).
- Hawley-Jones, T. J., Read, F. H., Cvejanovic, S., and King, G. C. (1992). *J. Phys. B* **25**, 2393.
- Kheifets, A. (1993). *J. Phys. B* **26**, 2053.
- Krause, M. O., Whitfield, S. B., Caldwell, C. D., Wu, J-Z., van der Meulen, P., de Lange, C. A., and Hansen, R. W. C. (1992). *J. Elect. Spectrosc. Relat. Phenom.* **58**, 79.
- Kuchiev, M-Y., and Sheinerman, S. A. (1989). *Sov. Phys. Usp.* **32**, 569.
- Kuchiev, M-Y., and Sheinerman, S. A. (1994). *J. Phys. B* **27**, 2943.
- Leung, K. T., and Brion, C. E. (1983). *Chem. Phys.* **82**, 87.
- Lohmann, B. (1991). *J. Phys. B* **24**, L249.
- Lohmann, B., Meng, X-K., and Keane, M. (1992). *J. Phys. B* **25**, 5223.
- Lower, J., and Weigold, E. (1989). *J. Phys. E* **22**, 421.
- Lower, J., and Weigold, E. (1990). *J. Phys. B* **23**, 2819.
- Lubell, M. S. (1994). *Z. Phys. D* **30**, 79.
- McCarthy, I. E., Pascual, R., Storer, P., and Weigold, E. (1989). *Phys. Rev. A* **40**, 3041.
- McCarthy, I. E., and Weigold, E. (1988). *Rep. Prog. Phys.* **51**, 299.
- McCarthy, I. E., and Shang, B. (1993). *Phys. Rev. A* **47**, 4807.

- McCarthy, I. E., and Weigold, E. (1991). *Rep. Prog. Phys.* **54**, 789.
- McDonald, D. G., and Crowe, A. (1992). *Z. Phys. D* **23**, 371.
- McDonald, D. G., and Crowe, A. (1993). *J. Phys. B* **26**, 2887.
- Pochat, A., Tweed, R. J., Doritch, M., and Peresse, J. (1982). *J. Phys. B* **15**, 2269.
- Samardzic, O., Braidwood, S. W., Weigold, E., and Brunger, M. J. (1993). *Phys. Rev. A* **48**, 4390.
- Samardzic, O., Hurn, J., Weigold, E., and Brunger, M. J. (1994). *Aust. J. Phys.* **47**, 703.
- Samardzic, O., Kheifets, A., Weigold, E., Shang, B., and Brunger, M. J. (1995). *J. Phys. B* **28**, 725.
- Sandner, W., and Völkel, M. (1984). *J. Phys. B* **17**, L597.
- Sewell, E. C., and Crowe, A. (1982). *J. Phys. B* **15**, L357.
- Sewell, E. C., and Crowe, A. (1984). *J. Phys. B* **17**, 2913.
- Shore, B. W. (1967). *Rev. Mod. Phys.* **39**, 439.
- Spears, D. P., Fischbeck, H. J., and Carlson, T. A. (1974). *Phys. Rev. A* **9**, 1603.
- Stefani, G., Avaldi, L., Lahmann-Bennani, A., and Duguet, A. (1986). *J. Phys. B* **19**, 3787.
- Svensson, S., Eriksson, B., Martensson, N., Wendin, G., and Gelius, U. (1988). *J. Elect. Spectrosc. Relat. Phenom.* **47**, 327.
- Tweed, R. J., and Langlois, J. (1986). *J. Phys. B* **19**, 3583.
- van den Brink, J. P., Nienhuis, G., van Eck, J., and Heideman, H. G. M. (1989). *J. Phys. B* **22**, 3501.
- Waterhouse, D. K., Flexman, J., and Williams, J. F. (1993). Abstracts 18th Int. Conf. on the Physics of Electronic and Atomic Collisions, p. 212 (Aarhus University: Aarhus).
- Weigold, E., Hood, S. T., and McCarthy, I. E. (1975a). *Phys. Rev. A* **11**, 566.
- Weigold, E., Noble, C. J., Hood, S. T., and Fuss, I. (1979). *J. Phys. B* **12**, 291.
- Weigold, E., Ugbabe, A., and Teubner, P. J. O. (1975b). *Phys. Rev. Lett.* **35**, 209.

